Terahertz-wave Integrated Circuits Based on Photonic Crystals

Kazuisao Tsuruda[1, 2], **Masayuki Fujita**[1], **Asako Suminokura**[1], **Masahiro Yata**[1], **Toshikazu Mukai**[2], **and Tadao Nagatsuma**[1]

[1]Graduate School of Engineering Science, Osaka University
1-3 Machikaneyama, Toyonaka, Osaka 560-8531, Japan
[2]Sensor Business Strategy Optical Device Research and Development Div.
ROHM Co., Ltd. 21, Saiin Mizosaki-cho, Ukyo-ku, Kyoto 615-8585, Japan

Abstract— We study a terahertz-wave integrated circuits based on a two-dimensional photonic crystal (PC) slab to manipulate terahertz waves with low loss. We demonstrate a PC waveguide with a low propagation loss (< 0.2 dB/cm). Based on this PC waveguide, we develop a diplexer using a directional coupler whose short length is comparable to the wavelength. We also fabricate a grating coupler as an interface of the waveguide to free space. Finally, the integration of terahertz diode chips into the waveguide is discussed. The propagation frequency band of the PC waveguide is successfully observed from the integrated device that uses a diode as a terahertz detector. We also achieve a 7.5-Gbit/s error-free terahertz-wave transmission using the device in the 0.3-THz band.

1. INTRODUCTION

Recently, the frequency band of terahertz electromagnetic waves (from 0.1 to 10 THz) has attracted much attention owing to its unique application possibilities such as spectroscopic sensing, non-destructive imaging, and ultra-broadband wireless communication [1]. However, most existing terahertz wave application systems and devices require the use of bulky and discrete components, including sources, detectors, hollow-core waveguides, and lenses. Size reduction of the devices and development of integration platform are required to build a terahertz wave integrated circuit (IC) in a thin, planar structure with low loss. As a terahertz integration platform, metal-based structures such as metallic transmission lines and electromagnetic metamaterials are being extensively studied [2–5]. However, the intrinsic absorption loss of metals in the terahertz frequency region is high and uncontrollable. We have proposed a photonic crystal (PC) slab consisting of a two-dimensional (2D) lattice of air holes formed in silicon (Si) as an alternative platform for terahertz wave manipulation [6]. This is because an ultralow-propagation-loss (less than sub dB/cm) waveguide for terahertz waves can be theoretically achieved if high resistivity (more than several kΩ· cm) Si is used [7]. Fig. 1 shows the schematic image of a terahertz-wave IC based on a PC slab, which consists of a waveguide [8], a diplexer [9], a grating coupler [10], and terahertz receiver [11] and transmitter mounted on a PC slab platform.

In this paper, we present the development of each component shown in Fig. 1. We estimate the propagation loss of the PC waveguide at 0.3-THz band, where various applications are being rapidly developed [1]. The compact diplexer is designed and fabricated for frequency-division communications. The grating coupler is used as an input/output interface in place of conventional antenna structures. We also discuss how terahertz waves confined in the dielectric PC waveguide can be efficiently coupled to diode devices. Finally, we demonstrate an error-free giga-bit transmission using the diode-integrated waveguide.

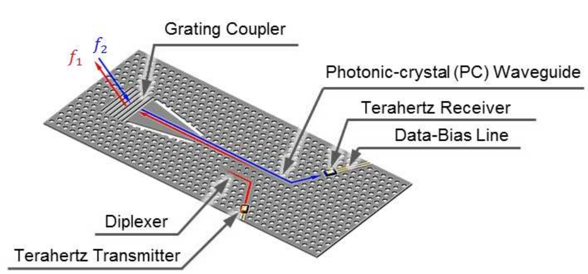

Figure 1: Schematic image of a terahertz-wave transceiver IC based on a PC platform.

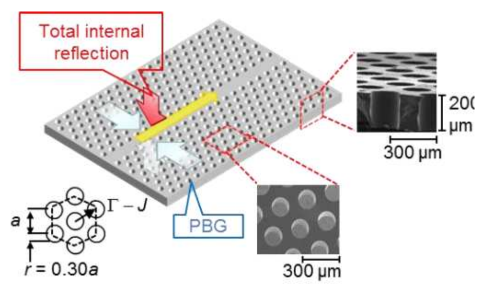

Figure 2: Schematic and pictures of the PC waveguide.

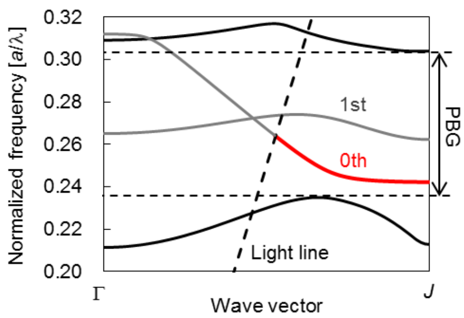

Figure 3: Dispersion diagram of the guided modes.

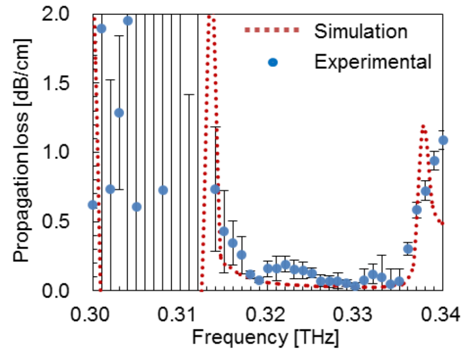

Figure 4: Frequency dependence of the propagation loss.

2. LOW-LOSS PC WAVEGUIDE

Figure 2 shows the schematic of a PC waveguide. The PC slab has a 2D triangular lattice of circular air holes in 200-μm-thick Si. The lattice constant a of the PC and air-hole radius r are set to 240 and 72 μm, respectively. The PC has 2D a photonic bandgap (PBG) effect where no propagation modes exist in the in-plane directions, as shown in Fig. 3. The line defect is introduced along the Γ-J direction. Fig. 3 shows the calculated dispersion curves of the guided modes. The dashed line is the light line, which corresponds to the dispersion in free space. Theoretically, no radiation loss is expected below the light line because the electromagnetic wave can be completely confined in both the vertical and in-plane directions by total internal reflection and the PBG effect, respectively [12]. The fundamental guided mode occurs from 0.242 of the normalized frequency. The waveguide was fabricated by photolithography and dry etching.

Figure 4 shows the measured propagation loss. The experimental results show good agreement with the simulation results calculated by the finite-difference time-domain method. Low propagation loss (< 0.2 dB/cm) is achieved in the PC waveguide from 0.318 to 0.335 THz where the non-leaky condition is satisfied. The 20-kΩ· cm high-resistivity Si contributes to the reduction of the absorption loss due to the free-carrier in Si. The propagation loss is one or two orders of magnitude smaller than that of typical metallic lines [2–4]. To the best of our knowledge, this value is also the smallest ever reported among various PC waveguides, including those in the light-wave region (~ 2 dB/cm) [13].

3. COMPACT DIPLEXER

A compact frequency selector that uses 2D PC cavities has been reported in the light-wave region [14]. However, achieving a broadband operation is difficult due to their resonant property. A directional coupler is a candidate to make broadband operation in contrast to the cavity-based structure. The coupling length and the interval between two waveguides are designed be $4a$ and two rows, respectively [9] as shown in Fig. 5. The length is comparable to the wavelength. Radius r' of the line defect is set to $0.23a$ for broadband operation. The waveguide width in port2 is narrower $0.15a$ to match the guided band of port1 in the operating band. Furthermore, the location of the holes in the port3 area is shifted $0.30a$ to improve the isolation of the bar and cross states. Fig. 6 shows the field distributions of the guided mode for the bar and cross states at 0.32 and 0.33 THz, respectively. Fig. 7 shows the experimental results of the transmission spectrum. The 3-dB bandwidth of cross state is 2.3-% of the operation frequency, which is over 10 times wider compared with that reported in the light-wave region [15]. The isolation of the cross and bar states is over 30 dB.

4. GRATING COUPLER

Using a grating coupler is one of the methods to realize an input/output interface in the circuit. Fig. 8 shows the schematic of the grating coupler. Period Λ, grating depth d, and number of period N are set to 600 μm, 200 μm, and five, respectively. We have successfully demonstrated the operation with a center frequency of 0.327 THz, as shown in Fig. 9. The 6% transmittance can be improved to $> 50\%$ by optimization of the grating parameters [10].

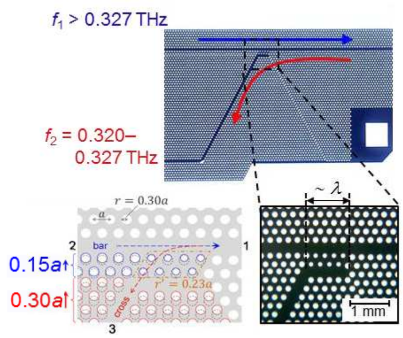

Figure 5: Schematic of the diplexer structure.

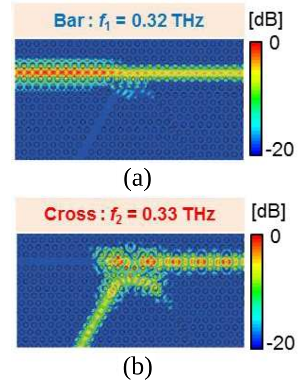

Figure 6: Electric-field intensity distributions.

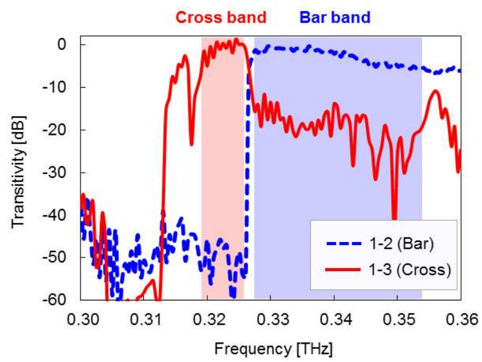

Figure 7: Transmission spectrum of the diplexer.

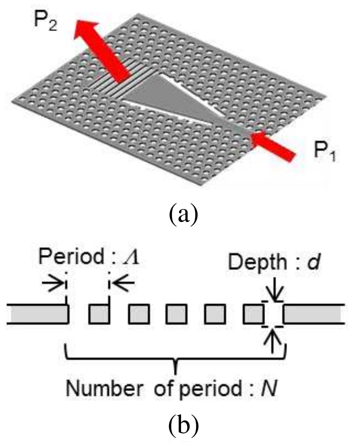

Figure 8: (a) Schematic of a grating coupler. (b) Structure parameters.

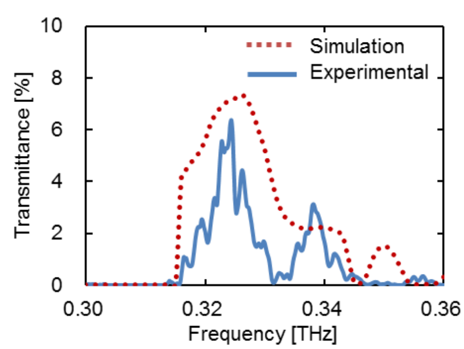

Figure 9: Transmission spectrum.

5. INTEGRATION WITH DIODE CHIP

We consider two schemes for the integration of diodes to the PC waveguide, as shown in Fig. 10. We apply a directional coupling method for the diode with a tapered slot antenna [11]. The diode chip is mounted on the PC waveguide with a center alignment of the diode to the PC waveguide. The guided terahertz wave in the PC waveguide is directionally coupled to the substrate of the chip and propagates in the tapered slot antenna, as shown in the simulated electric-field distribution in Fig. 10(a). In contrast, we use an end-fire coupling when the diode has simple two square electrodes. A diode chip is attached to the edge face of the PC waveguide. A terahertz wave propagating in the PC waveguide directly enters into the substrate of the diode chip through the junction normal to the propagation direction as shown in Fig. 10(b). Fig. 11 shows photographs of each fabricated module connected to a coplanar waveguide (CPW) and a coaxial connector.

Figure 12 shows the block diagram of the experimental setup for the frequency-response measurement. Signals in the range of 0.28–0.38 THz, modulated at 100 kHz by a −5-dBm output, were generated in which the millimeter-wave signals were multiplied nine times in the frequency range of 31–42 GHz. The generated terahertz wave was input via the tapered structure at the edge of the PC waveguide from the WR-3 rectangular waveguide [16]. The terahertz wave was detected by the diode, and the demodulated signal was transmitted to the coplanar strip line and coaxial connector and then measured by a spectrum analyzer. A direct-current voltage was applied to the diodes using a bias tee, and the output signal was extracted by the same CPW. Fig. 13 shows the measured frequency dependence of the normalized output signal power, which is demodulated by the diode detectors. In the theoretical propagation band of the PC waveguide, the intensity is increased by > 30 dB compared with the noise floor at 0.30 THz to 0.31 THz. This result demonstrates that the terahertz wave that propagates through the PC waveguide is successfully delivered to the electric devices. The end-fire coupling has wider broadband operation that the directional coupling. This difference is due to the multiple reflection inside the larger chip substrate of the directional coupling structure.

Finally, we demonstrated a terahertz-wave transmission using the fabricated detector module. Fig. 14 shows the block diagram of the experiment. The millimeter-wave was ON-OFF modulated using an intensity modulator, which was driven by a pulse pattern generator. The generated millimeter-wave was multiplied by nine times using a frequency multiplier. At the receiver side, the detected signal was amplified by a 25-dB-gain pre-amplifier with a bandwidth of 12 GHz, followed by waveform sharpening using a limiting amplifier. Fig. 15 shows the eye diagram at a bit rate of 7.5 Gbit/s with a frequency of 0.351 THz. Error-free transmission was confirmed using a bit error rate (BER) tester (BER $< 10^{-11}$). Terahertz-wave communication was successfully achieved via

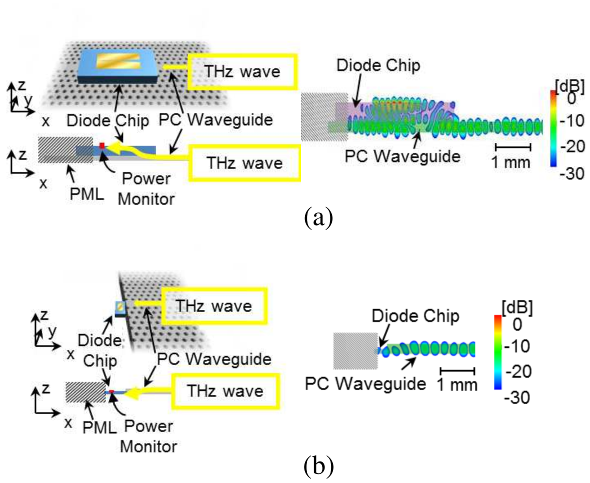

Figure 10: Schematics and simulated results of each coupling structure. (a) Directional coupling. (b) End-fire coupling.

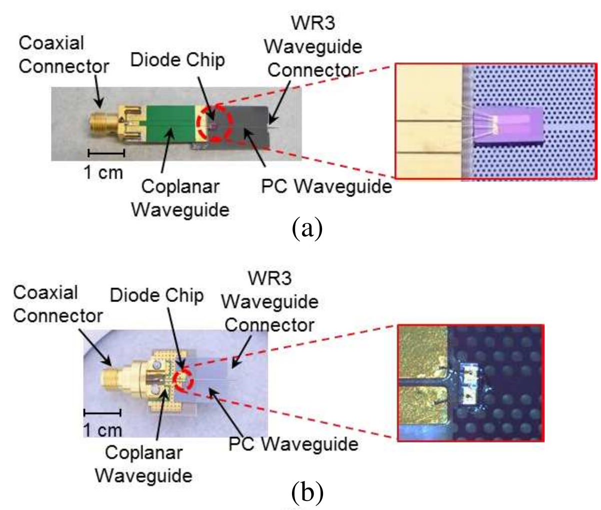

Figure 11: Photographs of each fabricated module.

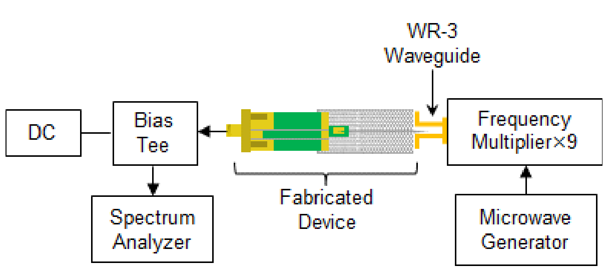

Figure 12: Block diagram for the measurement of the frequency response.

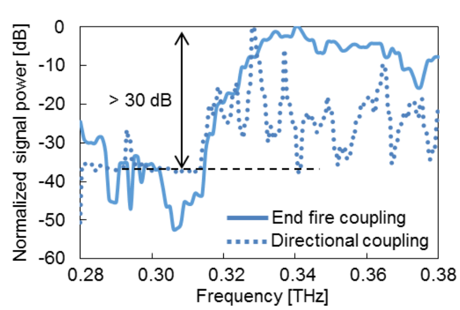

Figure 13: Measured frequency dependence of output signal power.

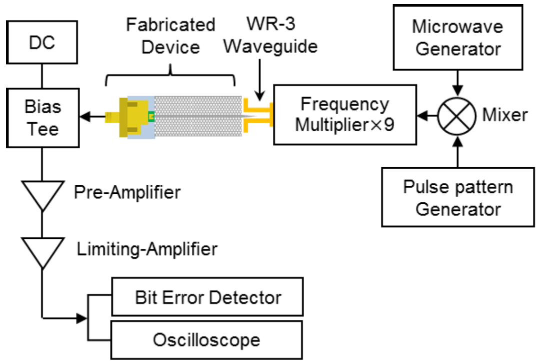

Figure 14: Block diagram for the terahertz communication experiment.

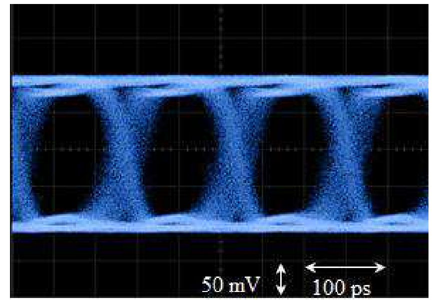

Figure 15: Measured eye diagram.

the integration of a Schottky Barrier diode chip with the PC waveguide.

6. CONCLUSION

We have presented terahertz-wave components using PC. We have developed a PC waveguide with very low propagation loss. On the basis of this PC waveguide, we have developed a diplexer using a small directional coupler. We fabricated a grating coupler for the waveguide as an input/output interface. We have successfully integrated terahertz diode detectors to the PC waveguide and evaluated the frequency characteristics at the 0.3-THz band. We have also demonstrated a 7.5-Gbit/s error-free terahertz transmission as a receiver module. In our future works, we plan to integrate a terahertz resonant tunneling diode (RTD) oscillator [17] with a PC waveguide for demonstration as a terahertz transceiver module. The important challenge would be the improvement of the coupling efficiency of the diode and PC waveguide. These efforts will lead to the realization of terahertz-wave ICs based on a PC that reduces the size of terahertz-wave systems for advanced information communication technologies.

ACKNOWLEDGMENT

This work was supported in part by the Strategic Information and Communications R&D Promotion Programme (SCOPE) from the Ministry of Internal Affairs and Communications of Japan, a Grant-in-Aid for scientific research from the Ministry of Education, Culture, Sports, Science and Technology of Japan, and the TEPCO Memorial Foundation.

REFERENCES

1. Nagatsuma, T., *IEICE Electron*, Exp. 8, 1127, 2011.
2. Frankel, M. Y., S. Gupta, J. A. Valdmanis, and G. A. Mourou, *IEEE Trans. Microwave Theory Tech.*, Vol. 39, No. 6, 910, 1991.
3. Heiliger, H. M., M. Nagel, H. G. Roskos, H. Kurz, F. Schnieder, W. Heinrich, R. Hey, and K. Ploog, *Appl. Phys. Lett.*, Vol. 70, No. 17, 2233, 1997.
4. Takase, K., T. Ohkubo, F. Sawada, D. Nagayama, J. Kitagawa, and Y. Kadoya, *Jpn. J. Appl. Phys.*, Vol. 44, No. 28, 1011, 2005.
5. Reinhard, B., O. Paul, and M. Rahm, *IEEE J. Sel. Top. Quantum Electron.* Vol. 19, 8500912, 2013.
6. Kakimi, R., M. Fujita, M. Nagai, M. Ashida, and T. Nagatsuma, *Nature Photon.*, Vol. 8, 657, 2014.
7. Ishigaki, T., M. Fujita, M. Nagai, M. Ashida, and T. Nagatsuma, *Proc. IEEE Photonics Conference*, 774, 2012.
8. Tsuruda, K., T. Ishigaki, A. Suminokura, R. Kakimi, M. Fujita, and T. Nagatsuma, *IEEE Int. Top. Meet. on Microw. Photon. (MWP2013)*, 9, 2013.
9. Yata, M., M. Fujita, and T. Nagatsuma, *Int. Top. Meet. Microw. Photon./Asia-Pacific Microw. Photon. Conf. (MWP/APMP2014)*, 40, 2014.
10. Suminokura, A., T. Ishigaki, M. Fujita, and T. Nagatsuma, *Asia-Pacific Radio Sci. Conf.*, DJ2b-3, 2013.

11. Suminokura, A., K. Tsuruda, T. Mukai, M. Fujita, and T. Nagatsuma, *Int. Top. Meet. Microw. Photon./Asia-Pacific Microw. Photon. Conf. (MWP/APMP2014)*, 419, 2014.
12. Fujita, M., S. Takahashi, Y. Tanaka, T. Asano, and S. Noda, *Science*, Vol. 308, No. 5726, 1296, 2005.
13. Notomi, M., T. Tanabe, A. Shinya, E. Kuramochi, H. Taniyama, S. Mitsugi, and M. Morita, *Opt. Express*, Vol. 15, No. 26, 17458, 2007.
14. Noda, S., A. Chutinan, and M. Imada, *Nature*, Vol. 407, 608, 2000.
15. Sugisaka, J., N. Yamamoto, M. Okano, K. Komori, and M. Itoh, *Jpn. J. Appl. Phys.*, Vol. 50, 32201, 2011.
16. Tailaert, D., F. V. Laere, M. Ayre, W. Bogaerts, D. V. Thourhout, P. Bienstman, and R. Baets, *Jpn. J. Appl. Phys.*, Vol. 45, No. 8A, 6071, 2006.
17. Asada, M., S. Suzuki, and N. Kishimoto, *Jpn. J. Appl. Phys.*, Vol. 47, 4375, 2008.